



EuroGEOSS Showcases: Applications Powered by Europe

S6P3 – Silesian Coal Basin Results



The e-shape project has received funding from the European Union's Horizon 2020 research and innovation programme under grant agreement 820852

List of Authors:

Maria Przyłucka ¹

Pablo Ezquerro ²

¹ Państwowy Instytut Geologiczny - Państwowy Instytut Badawczy, PGI

² Geological Survey of Spain, IGME-CSIC



The e-shape project has received funding from the European Union's Horizon 2020 research and innovation programme under grant agreement 820852



TABLE OF CONTENTS

TABLE OF CONTENTS	3
1 INTRODUCTION	4
2 PRODUCT 1: INSAR PROCESSING.....	5
3 PRODUCT 2: INSAR VALIDATION REPORT	7
3.1 AUXILIARY DATA	7
3.2 QUANTITATIVE VALIDATION.....	7
3.3 QUALITATIVE VALIDATION	8
4 PRODUCT 3: ACTIVE GEOHAZARD AREAS REPORT	9
4.1 PRE-ANALYSIS	9
4.2 MINING AREAS REPORT: ANALYSIS OF MINING DISTRICTS AND EVOLUTION OF THE EXTRACTED VOLUMES.....	10
5 PRODUCT 4: URBAN VULNERABLE AREAS REPORT.....	14
5.1 IDENTIFICATION OF INDUCED DISPLACEMENTS: DISPLACEMENT THRESHOLDS	14
6 REFERENCES.....	16

1 INTRODUCTION

Upper Silesian Coal Basin (USCB) is one of the most significant coal basins in Europe, located in the South of Poland (Fig. 1) with major cities Katowice, Sosnowiec, Gliwice, Zabrze and Bytom. Carboniferous hard coal underground exploitation has been conducted here since the XIX century. Nowadays, due to significant reduction of production since 1990 there are only around forty deposits exploited by thirty active hard coal mines, where longwall mining typically operates at depths reaching more than 1000 m. At the same time, Upper Silesia is a relatively big metropolitan area occupied by 37 towns with almost 3 million inhabitants. More than a century of mining activity have caused irreversible changes on the earth's surface over large areas. Among geohazards such as sinkholes, inundations, and landslides, the impact of subsidence is the most noticeable. According to the current estimates, the direct influence covers approx. 650 km² and indirect influence of the mining industry approx. 1000 km². The subsidence over a typical mining wall at a depth of 680 meters, thickness of 2.5 meters and 250 to 400 meters long, reaches up to 70% of the layer height, which corresponds to the largest vertical displacement from 0.75 to 2.0 m in the central part of the basin. Due to the use of many seams, vertical displacements in the area reach up to tens of meters in some places. For the greater part of the area, depressions reached 0.5-1.0 m, and in extreme cases, they were even 30-40 m. The most significant increase in subsidence was recorded in the 1970s, during intensive exploitation in the Bytom protection pillar. At that time, the average daily increments of subsidence of up to 5 mm were recorded. Vertical terrain displacements are monitored using classical geodetic methods and occasionally using differential analyzes of high-resolution numerical terrain models obtained by LIDAR. Levelling is the most popular subsidence monitoring method used in USCB. However, the main limitation of field-based monitoring techniques is the need for frequent field observations, which will increase the monitoring costs. The rapid development of remote sensing Earth observation methods allows them to detect changes in the terrain surface. Among these methods, Synthetic Aperture Radar Interferometry (InSAR) has proved to be the most useful. Studies on ground subsidence over USCB detected by InSAR are presented for example by: Perski 1998, Graniczny et al. 2007, Przyłucka et al. 2014, Przyłucka et al. 2015, Ilieva et al. 2019, Pawłuszek-Filipiak and Borkowski 2020, Sopata et al. 2020, Witkowski et al. 2021, Dwornik et al. 2021).

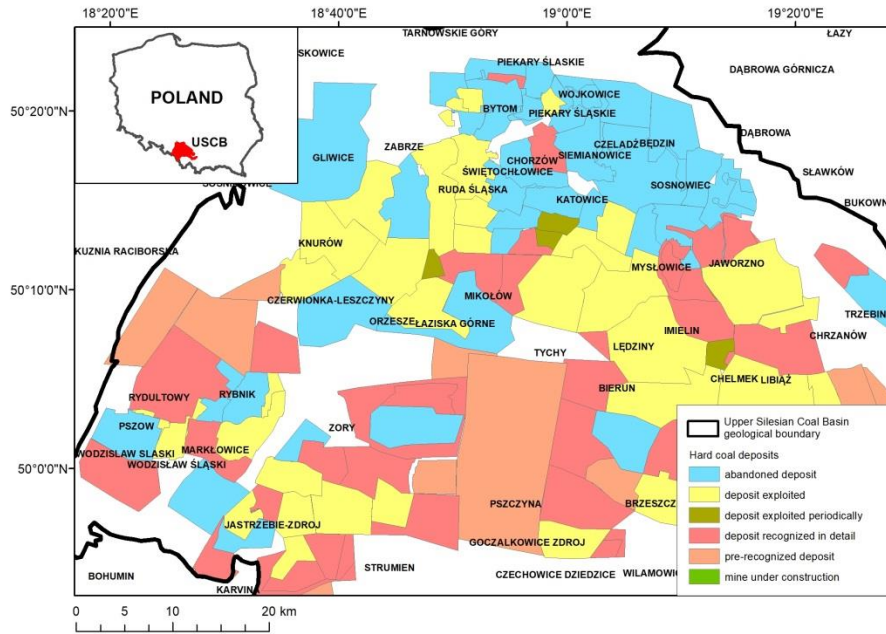


Figure 1: Distribution and activity of the Silesian Coal Basin mining districts.

e-Shape products provide advanced analysis useful to monitor, understand and reduce the effects of the associated geohazard: subsidence due to mining activities.

2 PRODUCT 1: INSAR PROCESSING

Satellite radar differential interferometry (DInSAR) is a geodesic technique that allows to remote sense small displacements of the terrestrial surface by analysing the phase differences between pairs of single look complex (SLC) SAR images. There are two methods to create the stack of interferograms. The first one uses a single reference SAR image (Single master). The second one uses a small baseline configuration, where a denser interferogram network is created linking multiple SAR images (Multi-master). The criterion to select the punctual targets in the interferograms can be simplified in amplitude and coherence methods. Amplitude selection methods work at full resolution and limit the interferometric processing only to those pixels that behave consistently over a long period of time (PS). Coherence based methods use distributed scatters (DS), or in other words, areas whose scatter properties are not altered with time, which requires a multilook that lowers the resolution. The Small Baseline Subset (SBAS) approach (Berardino et al., 2002) is a seminal work that proposes a complete advanced DInSAR procedure using small baselines to limit the spatial decorrelation, multilooked data to reduce phase noise and a coherence based selection criterion.

To deal with the current scenario characterized by huge SAR archives relevant to the present and future SAR missions, a parallel computing solution for the SBAS processing chain (P-SBAS) was developed (Casu et al., 2014). This step forward in optimizing computing performance was particularly suitable for web service implementation and handling big data volumes. Indeed, the P-SBAS algorithm was integrated within the Grid Processing on Demand (G-POD) environment by CNR IREA into the ESA's Geohazards Exploitation Platform (GEP). The developed on-demand web tool, which is specifically addressed to scientists that are non-expert in DInSAR data processing, permits to set up an efficient on-line P-SBAS processing service to produce surface deformation mean velocity maps and time series in an unsupervised manner (De Luca et al., 2015). The other Thematic Application used was the FASTVEL algorithm which was developed by TRE-Altamira for generating differential interferograms and PSI-based mean displacement velocity maps (not time series) from a set of Sentinel-1 images.

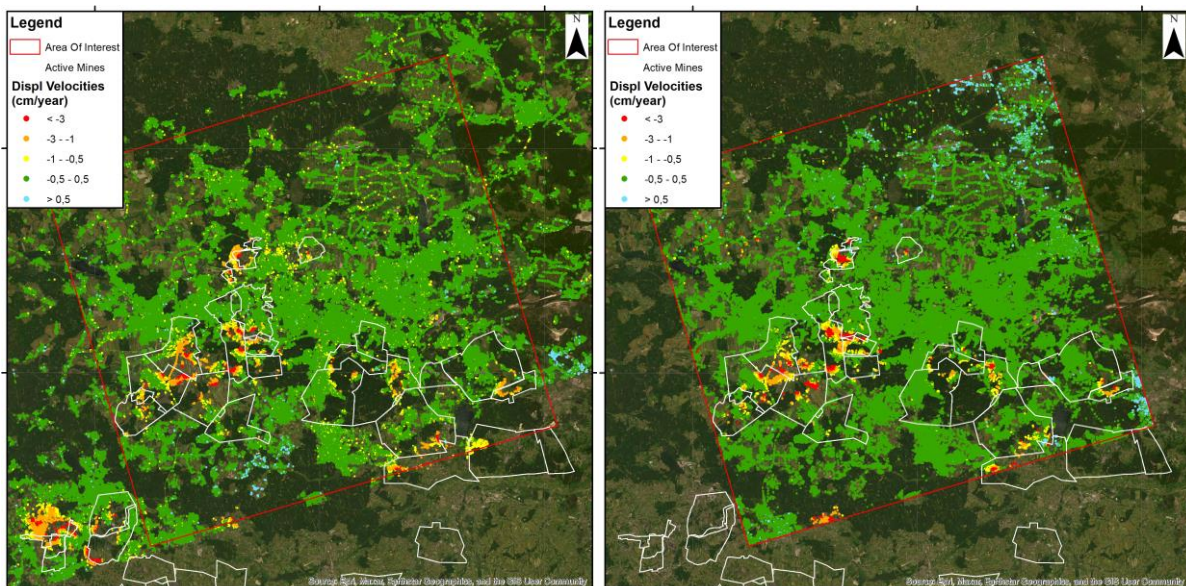


Figure 2: Mean LOS displacement during the studied period using P-SBAS (left) and FASTVEL (right).

P-SBAS processing used 216 images from March 2015 to September 2019 from 175 Sentinel-1 ascending track obtaining both displacement velocities and time series. FASTVEL results are more limited including only 71 images from February 2015 to March 2017 in the same track and geometry, making them fully comparable and allowing cross-validation.

InSAR results show a good general stability with a stability threshold of 0.5 cm/year. Maximum displacements are located around Katowice city, concentrated over the active mining districts, with values until 15 cm/year and 11 cm/year in FASTVEL and P-SBAS respectively.

Both InSAR results present coherent displacements with similar stability thresholds which validation will be analyzed in section 3. The magnitude of the displacements is significantly greater than stability thresholds, improving their interpretation.

3 PRODUCT 2: INSAR VALIDATION REPORT

Validation report aim to provide validation to the InSAR data based on complementary data provided by other measurement techniques. Those cases where that kind of data are not available, auxiliary data related to the possible trigger of the displacement can be used.

3.1 Auxiliary data

Silesian coal basin lacks of in-situ monitoring data deployed over the area but since two time coincident InSAR results from different processing algorithms are available, they can be cross-validated. Location of the active mining districts provided by the stakeholders also allow to perform a spatial qualitative validation.

3.2 Quantitative Validation

Following the e-shape proposed methodology, a Level 2 quantitative validation can be carried on using displacement velocities from P-SBAS and FASTVEL InSAR data. Through interpolation of the InSAR data using a IDW algorithm, both datasets are compared resulting in a Root Mean Square Error (RMSE) of 0.55 cm/year, around their stability thresholds. Comparing RMSE with the maximum displacements this error only signifies a 5% of the studied phenomenon.

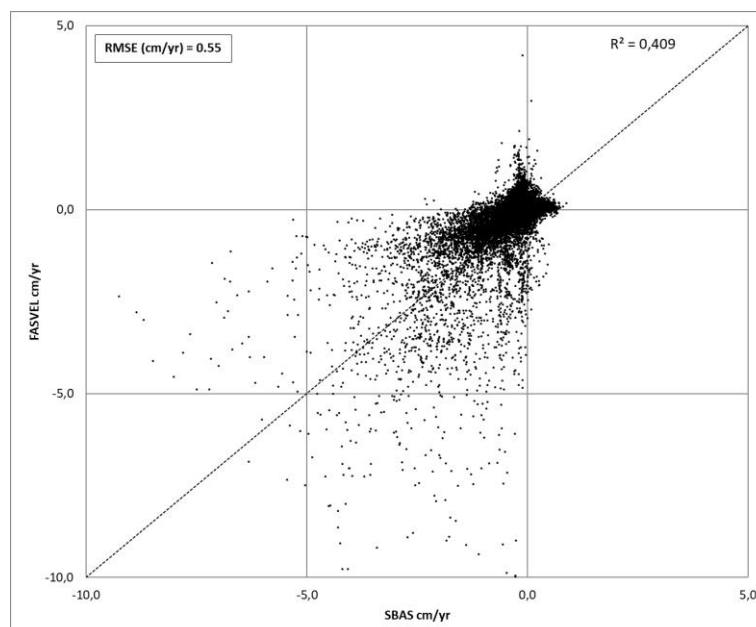


Figure 3: Comparison of the P-SBAS and FASTVEL velocities.

Using the methodology proposed by Navarro-Hernández et al. (2022) that compares relative RMSE and R^2 (0.41) (Fig. 3) the values of Silesian coal basin presents a “Good accuracy” validation result (RMSE < 30% and $0.4 < R^2 < 0.8$)

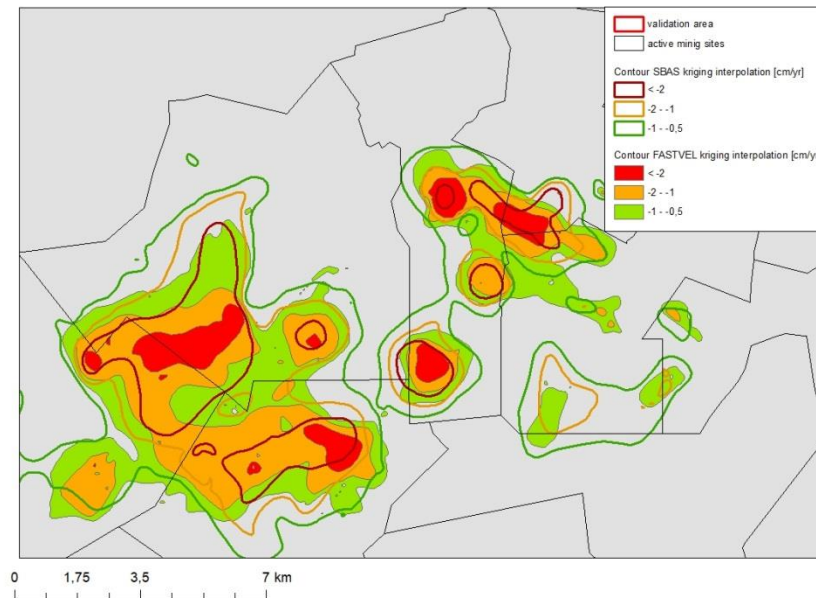


Figure 4: Spatial comparison of the displacement velocities detected by FASTVEL (polygons) and P-SBAS (lines)

Halfway between quantitative and qualitative validation, spatial comparison provides a good insight about the differences and allow to detect problematic areas. In this case study both datasets revealed a good coherence between them with slightly higher values in the P-SBAS results that can be explained by the differences in the processed time span and possible advances in the mining activities during the period (Fig. 4).

3.3 Qualitative Validation

Qualitative validation uses of the location of the mining districts, differentiated by their activity status to compare it with the location of the active areas. All of the 28 districts considered active during the period have revealed displacements away from satellite (Fig. 5), meanwhile only 3 of the 54 designed as inactive present that behaviour (considering only those PSs that show significant values). Most of the last category are in the vicinity of active ones that generate displacements in the surrounding area.

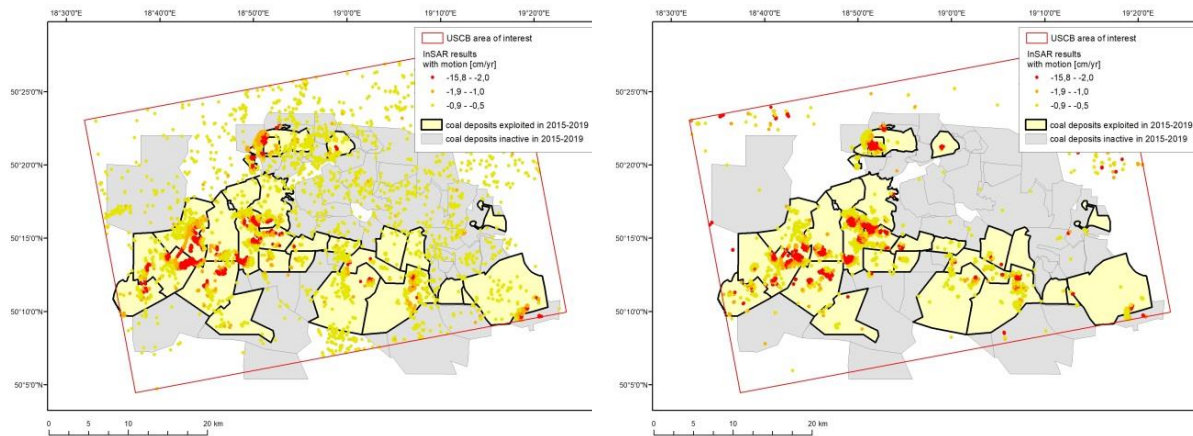


Figure 5: InSAR displacements and location of the exploited and inactive mining districts. SBAS results (left) and FASTVEL results (right).

4 PRODUCT 3: ACTIVE GEOHAZARD AREAS REPORT

Usually, InSAR processing generates thousands of points over the stability thresholds. Those points could be related to a geohazard or just noisy areas due to acquisition and processing challenges associated to the technique. Even in this case study the expected trigger mechanism is well defined, the processed area also covers other areas that could show other geohazards.

4.1 Pre-analysis

PSBAS InSAR results over the Silesian Coal Basin contains near 190642 points, with several areas over the displacement threshold that should be identified and, even they are not the main focus of the work, pre-analysed. In order to do so, ADA tool has been implemented to extract the main areas that concentrates significant displacement points. In this case clusters of more than 5 points over the threshold (± 0.5 cm/year) were selected, detecting 104 active clusters. 69 of them are located over mining districts and another 13 nearer than 1 km, which main displacement trigger is probably related to their activities (Fig. 6).

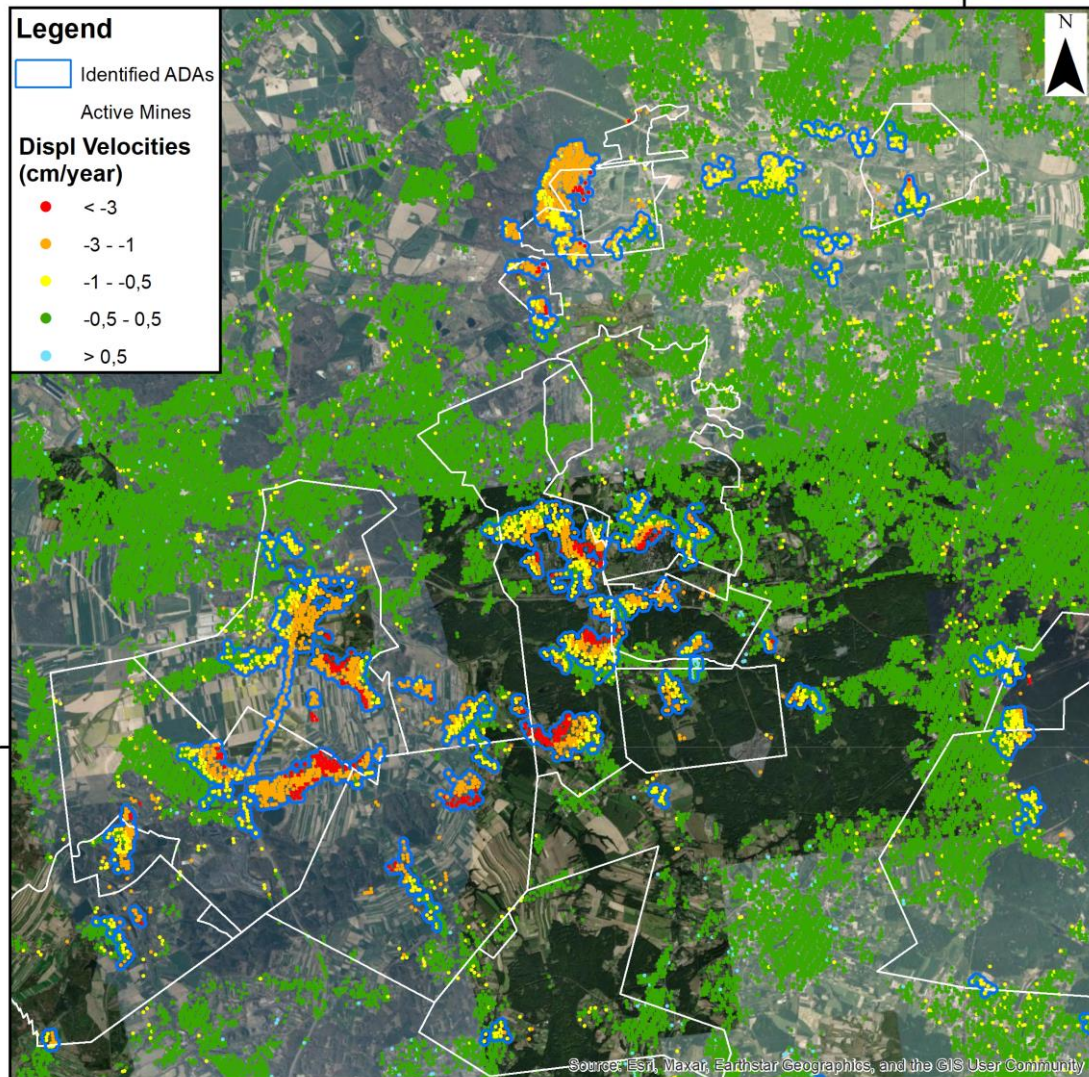


Figure 6: Active areas with more than 5 points over the main subsidence area

Other tools designed to aggregate and consolidate ADAs generated by the same triggering process have been tested. Results were not adequate due to the high variability of the mining areas that reduce the spatial continuity of the InSAR results but also the spatially limited affection of this kind of activities.

4.2 Mining Areas Report: Analysis of mining districts and Evolution of the extracted volumes

The most important geohazard of the area is subsidence due to mining activities. In this case the spatial and temporal relationship between the extractive activity and subsidence is analysed. Both tools applied in this part, Analysis of mining districts and Evolution of the extracted volumes, will help to achieve this target.

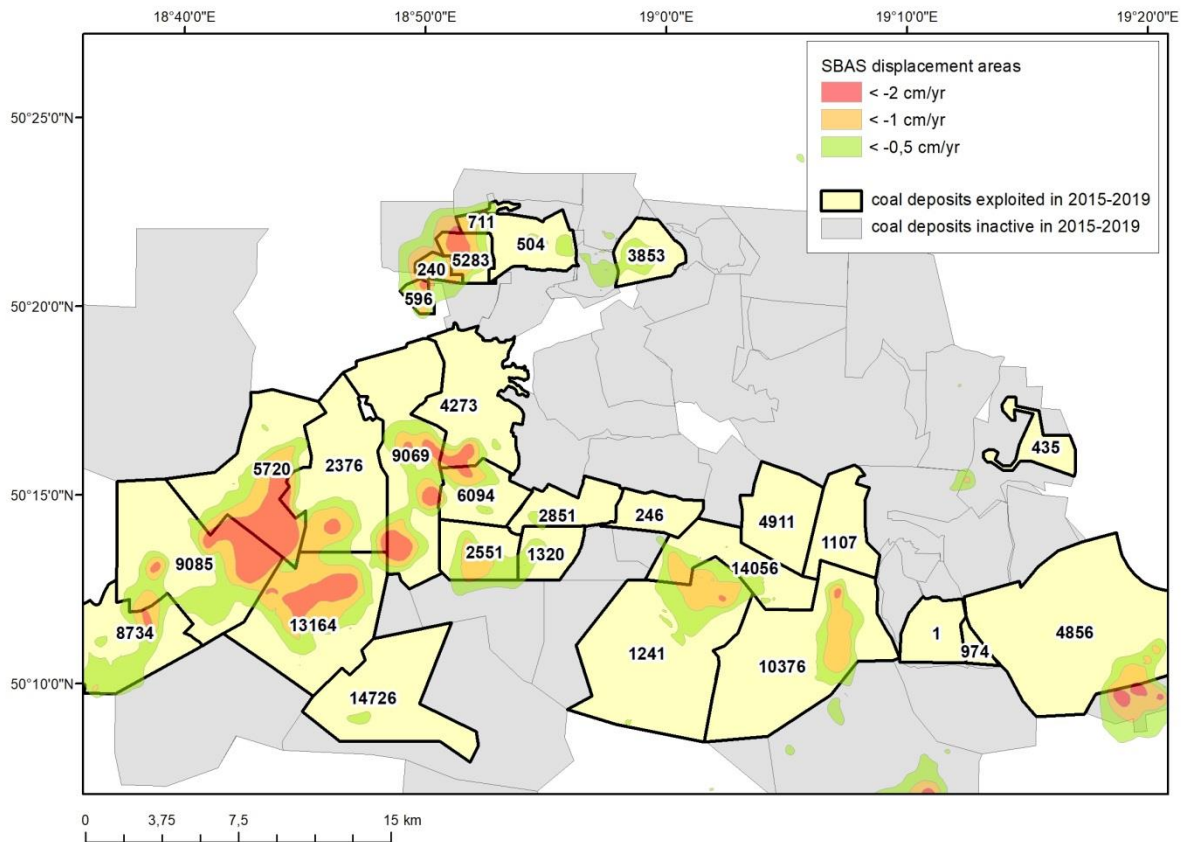


Figure 7: Coal deposits with displacements over the stability threshold. The numbers indicated sum of tons of coal exploited in the period 2014-2018.

First, the location of the mining districts has been compared with the InSAR-derived displacements to detect their activity and then compared with the reported as active (Fig. 7). Results using the displacement mean velocities show a clear correlation between the activity and detected subsidence. 28 districts were considered as active meanwhile 28 present InSAR displacements, with a 100% of coincidence. Taking into account that displacements due to mining activities are very spatially limited, analysis of the displacement evolution away from the mining district are not appropriate to study this area.

Within the 27 coal deposits that were exploited at least one year in the SBAS time span (2014-2019), the kilotons of coal exploited each year were compared with the average accumulated displacements. For each deposit all PSI points from SBAS dataset were selected and averaged their time series values for each date.

Results obtained revealed a good coherence between both time series in 24 of the 27 districts with three main differential behaviours (Tab. 1). One of them is related to areas where coal extractions are near constant, generating a continuous subsidence pattern in the areas (Fig. 8).

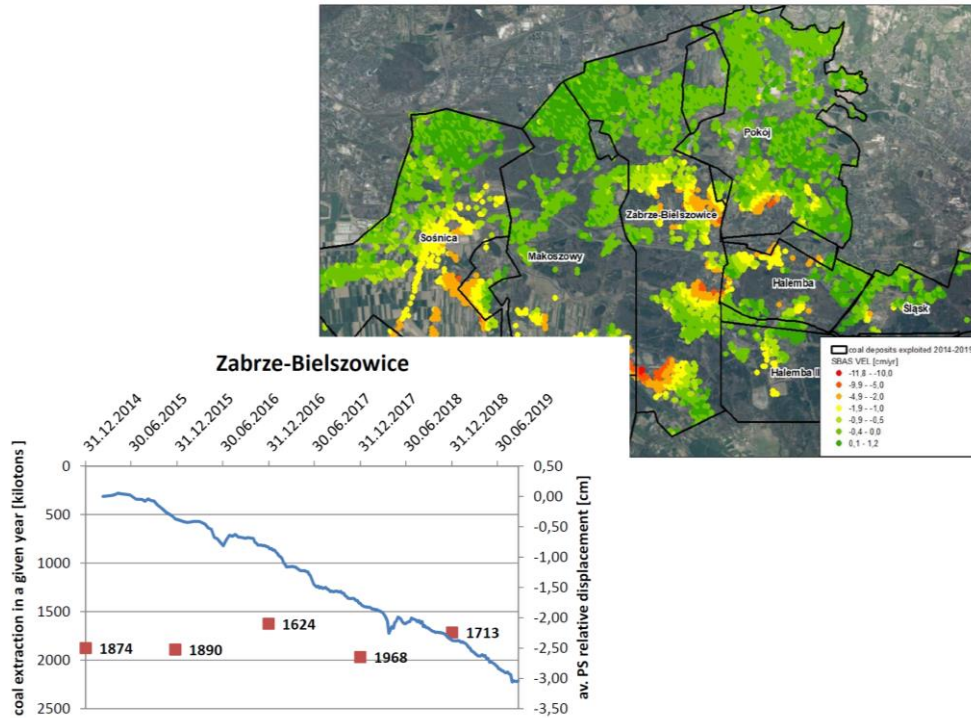


Figure 8: Mean velocity displacements, time series and coal extracted in the Zabrze-Bielszowice mining district.

Other areas are characterized by a slow declining trend associated to low extractions that presented an acceleration associated to a rising extractive activity (Fig. 9).

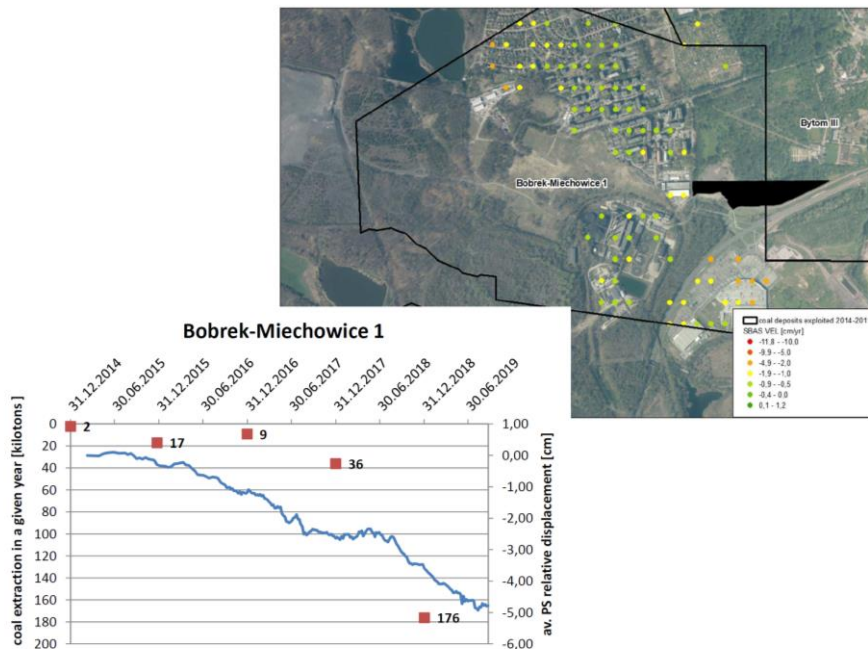


Figure 9: Mean velocity displacements, time series and coal extracted in the Bobrek-Miechowice 1 mining district.

Last, the opposite situation has been detected. Very active areas cease the productive activity with a consequent reduction of the displacements (Fig. 10).

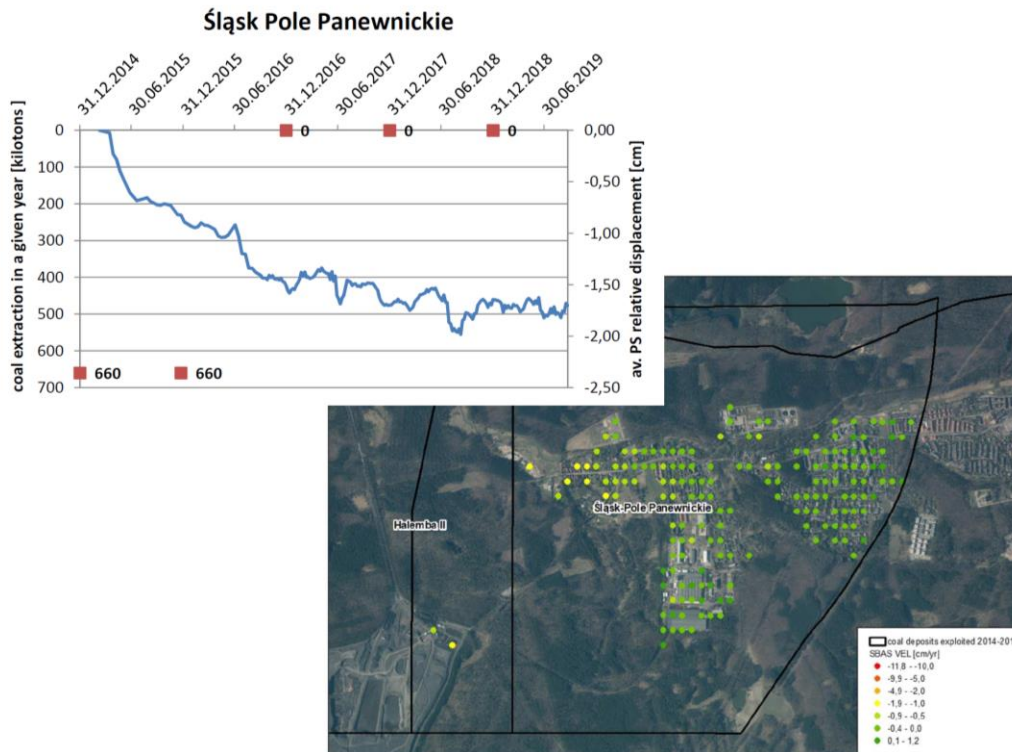


Figure 10: Mean velocity displacements, time series and coal extracted in the Śląsk Pole Panewnickie mining district.

Continuous	10
Acceleration	5
Stabilization	9
Anomalous	3

Table 1: Number of districts classified using the Time Series typology

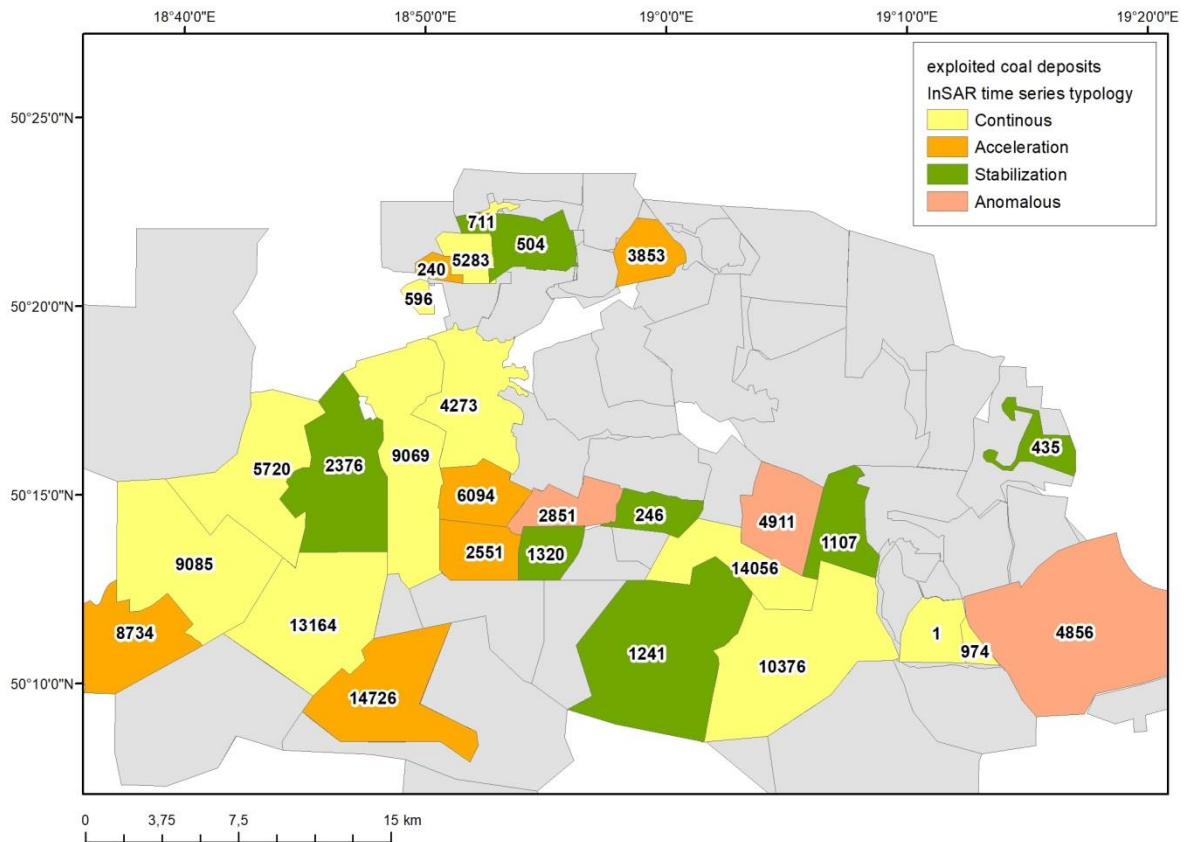


Figure 11: Location and classification of the districts depending on the Time Series typology

Table 1 and Figure 11 synthesize the results of this classification, with 10 districts showing a continuous trend, 5 presenting acceleration patterns and 9 corresponding to deaccelerating areas. This analysis allows to decision-makers to understand the status and trends of the different regions focusing on those with more expected problems.

5 PRODUCT 4: URBAN VULNERABLE AREAS REPORT

This product is very dependent on the available information, especially the existence of specifically designed campaigns to detect damages in the structures of the basin. In this study area, this kind of campaigns has not been carried on, so fragility curves are impossible to be calculated. Despite that, the region provided terrain deformation indexes used to defined the mining category.

5.1 Identification of induced displacements: Displacement Thresholds

As a mining area with a long history, in Upper Silesia three terrain deformation indexes are used to defined the mining category: tilt, curvature radius and horizontal deformation. The classification of the

influence of mining on the terrain surface is applied depending on the observed deformations (Tab. 2). The higher the category, the greater the degree of the damage risk. Category 0 means no risk, category V excludes any buildings.

category	The ranges of the terrain deformation indexes		
	tilt T [mm/m, ‰]	curvature radius R [km]	horizontal deformation ϵ [mm/m, ‰]
0	0,0 - 0,5	>40	0,0 - 0,3
I	0,5 - 2,5	40 - 20	0,3 - 1,5
II	2,5 - 5,0	20 - 12	1,5 - 3,0
III	5,0 - 10,0	12 - 6	3,0 - 6,0
IV	10,0 - 15,0	6 - 4	6,0 - 9,0
V	>15	<4	>9,0

Table 2: Silesian Coal Basin classification of the influence of mining on the terrain surface

From the InSAR data and the results obtained from the interpolation, it is possible to calculate the slope formed in the analyzed period and compare it with the thresholds for individual mining categories. However, both InSAR sets do not present subsidence that would reflect a mining category greater than 0. The SAR data processed in SBAS and Fastvel techniques do not allow the determination of true deformation, they are underestimated and the centres of the resulting basins are underestimated.

A mathematical approach was therefore adopted to categorize the impact of the mine based on InSAR data. The interpolated values are divided into 4 zones of mine influence, where:

- zone 0 <0.5 cm/yr (no influence)
- zone I 0.5 cm/yr – apx. st. dev.,
- zone II 1.0 cm/yr – 2*st.dev,
- zone III – 2.0 cm/yr which is known as a threshold value for the building structure

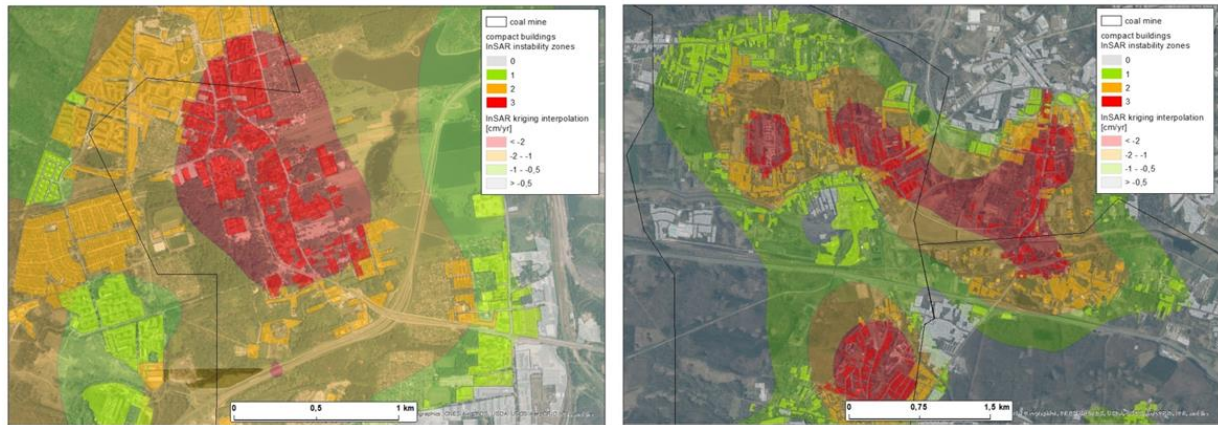


Figure 12: Accumulated displacements of each cadastral plot. Focus on the areas with the highest subsidence.

zone	number of objects	area [sq km]
0	52611	530,11
I	1971	15,97
II	1507	13,15
III	1381	11,04

Table 3: Building blocks and area affected by the different terrain deformation zones

In general, the basin displacements do not overtake the designed as without influence (Zone 0) in an 91.55% of the cadastral plots. The remaining 8.45%, a 6.05% are over areas in Zone I or II where significant displacements could be detected. Only 1381 (2.4%) buildings are over the Zone 3 threshold where should be monitored and damage detection campaigns planned. The most affected areas are located in the municipalities: Gierałtowice, Knurów, Mikołów, Bieruń, Chełm Śląski, Łędziny, Bytom, Katowice, Jaworzono, Myslowice, Ruda Śląska, Zabrze.

6 REFERENCES

Dwornik M, Porzycka-Strzelczyk S, Strzelczyk J, Malik H, Murdzek R, Franczyk A, Bała J, 2021. Automatic Detection of Subsidence Troughs in SAR Interferograms Using Mathematical Morphology. *Energies*, 14(22), 7785.

Graniczny M, Kowalski Z, Leśniak A, Czarnogórska M, Piątkowska A, 2007. Analysis of the PSI data from the Upper Silesia – SW Poland. The International Geohazard Week 5–9 November 2007 ESA-ESRIN Frascati Rome, Italy. The International Forum on Satellite EO and Geohazards: 17.

- Ilieva M, Polanin P, Borkowski A, Gruchlik P, Smolak K, Kowalski A, Rohm W, 2019. Mining deformation life cycle in the light of InSAR and deformation models. *Remote Sensing*, 11(7), 745.
- Pawluszek-Filipiak K, Borkowski A, 2020. Comparison of PSI and DInSAR approach for the subsidence monitoring caused by coal mining exploitation. *The International Archives of Photogrammetry, Remote Sensing and Spatial Information Sciences*, 43, 333-337.
- Perski Z, 1998. Applicability of ERS-1 and ERS-2 InSAR for land subsidence monitoring in the Silesian coal-mining region, Poland. *International Archives of Photogrammetry and Remote Sensing*, 32, 555-558.
- Przyłucka M, Graniczny M, Herrera G, 2014. Investigating strong mining-induced ground subsidence with X-band SAR interferometry in Upper Silesia in Poland. 5th EARSeL Workshop on Remote Sensing and Geology "Surveying the GEOsphere" 104 Warsaw, Poland, 19th – 20th June, 2014.
- Przyłucka M, Herrera G, Graniczny M, Colombo D, Béjar-Pizarro M, 2015. Combination of Conventional and Advanced DInSAR to Monitor Very Fast Mining Subsidence with TerraSAR-X Data: Bytom City (Poland). *Remote Sensing* 2015, 7(5), 5300-5328.
- Sopata P, Stoch T, Wójcik A, Mrocheń D, 2020. Land Surface Subsidence Due to Mining-Induced Tremors in the Upper Silesian Coal Basin (Poland)—Case Study. *Remote Sensing*, 12(23), 3923.
- Witkowski W T, Mrocheń D, Sopata P, Stoch T, 2021. Integration of the Leveling Observations and PSInSAR Results for Monitoring Deformations Caused by Underground Mining. In 2021 IEEE International Geoscience and Remote Sensing Symposium IGARSS (pp. 6614-6617). IEEE.
- Casu, F., Elefante, S., Imperatore, P., Zinno, I., Manunta, M., De Luca, C., and Lanari, R., 2014, SBAS-DInSAR parallel processing for deformation time-series computation: *IEEE Journal of Selected Topics in Applied Earth Observations and Remote Sensing*, v. 7, no. 8, p. 3285-3296.
- Berardino, P., Fornaro, G., Lanari, R., and Sansosti, E., 2002, A new algorithm for surface deformation monitoring based on small baseline differential SAR interferograms: *Geoscience and Remote Sensing, IEEE Transactions on*, v. 40, no. 11, p. 2375-2383.
- De Luca, C., Cuccu, R., Elefante, S., Zinno, I., Manunta, M., Casola, V., Rivolta, G., Lanari, R., and Casu, F., 2015, An on-demand web tool for the unsupervised retrieval of earth's surface deformation from SAR data: The P-SBAS service within the ESA G-POD environment: *Remote Sensing*, v. 7, no. 11, p. 15630-15650.